

## Protective effects of $\beta$ - nicotinamide adenine dinucleotide against motor deficits and dopaminergic neuronal damage in a mouse model of Parkinson's disease



Chang Shan<sup>a</sup>, Yan-ling Gong<sup>b</sup>, Qian-qian Zhuang<sup>b</sup>, Yan-fang Hou<sup>a</sup>, Shu-min Wang<sup>a</sup>, Qin Zhu<sup>a</sup>, Guo-rui Huang<sup>a</sup>, Bei Tao<sup>a</sup>, Li-hao Sun<sup>a</sup>, Hong-yan Zhao<sup>a</sup>, Sheng-tian Li<sup>b,\*</sup>, Jian-min Liu<sup>a,\*\*</sup>

<sup>a</sup> Department of Endocrine and Metabolic Diseases, Rui-jin Hospital, Shanghai Jiao Tong University School of Medicine, Shanghai Clinical Center for Endocrine and Metabolic Diseases, Shanghai Institute of Endocrine and Metabolic Diseases, Shanghai 200025, China

<sup>b</sup> Bio-X Institutes, Key laboratory for the Genetics of Developmental and Neuropsychiatric Disorders (Ministry of Education), Shanghai Key Laboratory of Psychotic Disorders, Brain Science and Technology Research Center, Shanghai Jiao Tong University, Shanghai 200240, China

### ARTICLE INFO

#### Keywords:

$\beta$ -Nicotinamide adenine dinucleotide  
Parkinson's disease  
Dopaminergic neuronal damage  
Oxidative stress  
Mitochondrial dysfunction

### ABSTRACT

The level of nicotinamide adenine dinucleotide (NAD) decreases in Parkinson's disease (PD), and its reduction has been reported to be involved in many age-associated neurodegenerative pathologies. Thus, we investigated whether NAD replenishment is beneficial in a 6-hydroxydopamine (6-OHDA)-induced mouse model of PD. Preinjection with NAD in the striatum ameliorated motor deficits and dopaminergic neuronal damage in the substantia nigra and striatum of a mouse model of PD. Moreover, preincubation with NAD protected PC12 cells against the loss of cell viability, morphological damage, oxidative stress and mitochondrial dysfunction caused by 6-OHDA. These results add credence to the beneficial role of NAD against parkinsonian neurodegeneration in mouse models of PD, provide evidence for the potential of NAD for the prevention of PD, and suggest that NAD prevents pathological changes in PD via decreasing mitochondrial dysfunctions.

### 1. Introduction

Parkinson's disease (PD) is a common age-related neurodegenerative disease that is characterized by canonical movement disorders and increasingly recognized nonmotor dysfunctions. Clinically, PD is dominated by motor dysfunction, including bradykinesia, tremor, rigidity and postural instability, that responds well to dopaminergic replacement therapy (Calabresi et al., 2013). However, current pharmacological treatments for PD provide only partial symptomatic relief and do not prevent progressive dopaminergic neurodegeneration in PD patients (Zhou et al., 2016). Therefore, new strategies are needed to prevent and treat this complex disease.

Dopaminergic neuronal degeneration in the substantia nigra (SN), along with the consequent severe dopaminergic denervation of the striatum (ST), which trigger a series of functional changes that affect the organization of the basal ganglia circuitry, are believed to be the cardinal pathological features of PD (Fearnley et al., 1991) (Dauer et al., 2003). Ameliorating or delaying dopaminergic neuronal

degeneration may be the keystone of PD therapeutics. Over the past decades, the course of neurodegeneration in PD has been understood to involve mitochondrial defects, oxidative stress, glutamate toxicity, genetic factors, and apoptosis (Blandini et al., 2000; Anderson et al., 2014). In particular, it has been found that a reduced level of nicotinamide adenine dinucleotide (NAD) may cause mitochondrial dysfunction (Verdin, 2015), DNA repair defects (Fang et al., 2017) and neuronal death (Alano et al., 2010; Zhou et al., 2015), resulting in many age-associated neurodegenerative pathologies (Imai et al., 2014). Based on the fact that PD is a common age-related disease involving NAD<sup>+</sup> depletion (Fang et al., 2017), it is highly possible that NAD<sup>+</sup> replenishment may protect against dopaminergic neurodegeneration in PD.

NAD is a dinucleotide consisting of two nucleotides joined by their phosphate groups, and it exists in two forms: the oxidized form (NAD<sup>+</sup>) and the reduced form (NADH). In addition to being an enzyme cofactor that mediates hydrogen transfer during redox reactions (Berger et al., 2004), it also serves as a cosubstrate for NAD<sup>+</sup>-consuming enzymes, including sirtuins, poly-ADP-ribose polymerases (PARPs), and CD38/

\* Correspondence to: S.-T. Li, Bio-X Institutes, Shanghai Jiao Tong University, No.800 Dongchuan Road, Shanghai 200240, China.

\*\* Correspondence to: J.-M. Liu, Department of Endocrine and Metabolic Diseases, Rui-jin Hospital, Shanghai Jiao Tong University School of Medicine, No.197 Ruijin Er Road, Shanghai 200025, China.

E-mail addresses: [lstian@sjtu.edu.cn](mailto:lstian@sjtu.edu.cn) (S.-t. Li), [ljm10586@rjh.com.cn](mailto:ljm10586@rjh.com.cn) (J.-m. Liu).

<https://doi.org/10.1016/j.pnpbp.2019.109670>

Received 22 December 2018; Received in revised form 6 May 2019

Available online 17 June 2019

0278-5846/ © 2019 Published by Elsevier Inc.

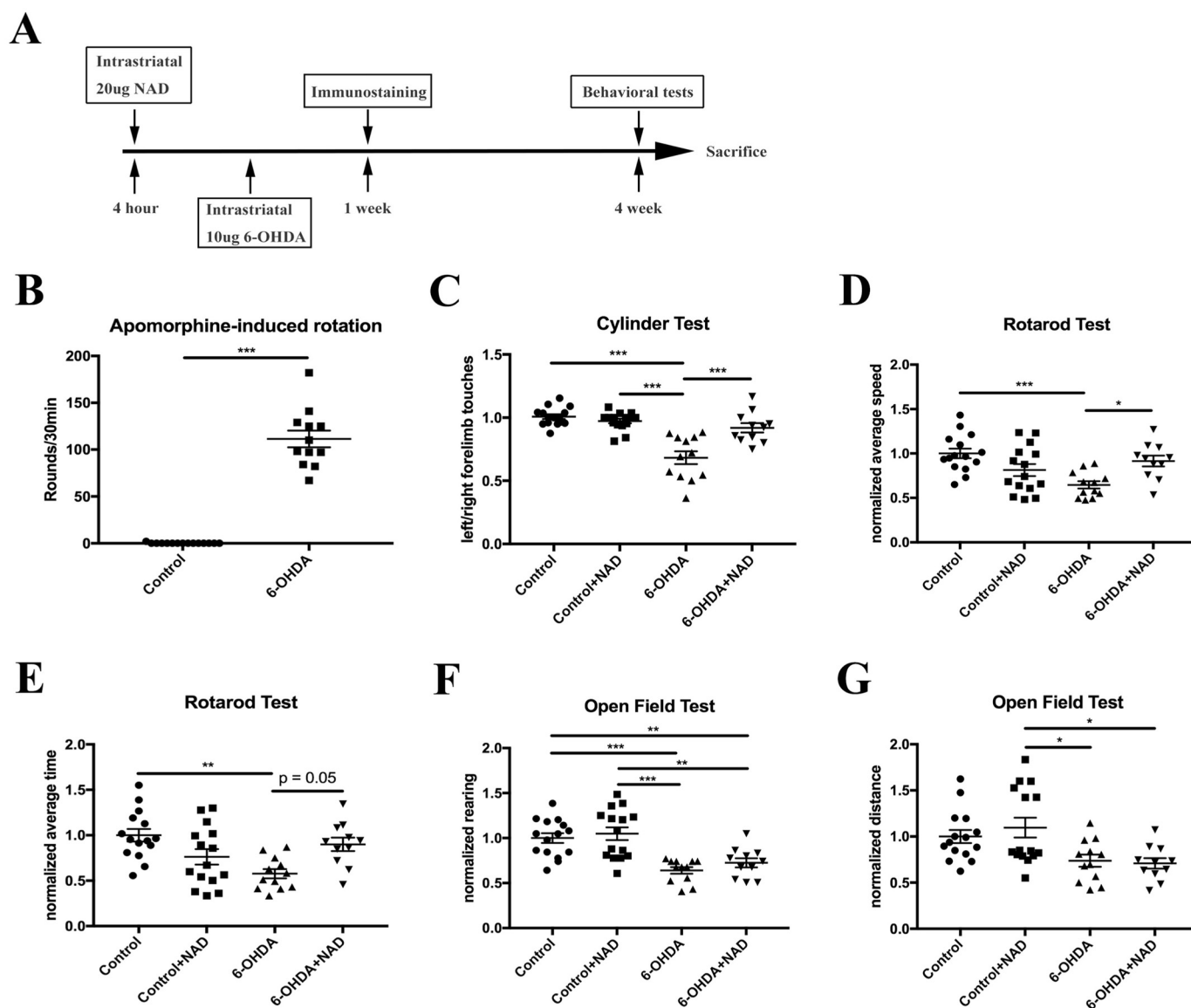


**Fig. 1.** NAD preadministration ameliorated motor deficits in PD mice. The experimental schedule for NAD intervention in the 6-OHDA-lesioned PD mouse model (A). Apomorphine-induced rotation (B) was used to evaluate the establishment of 6-OHDA-induced PD in the mice. The cylinder test (C), rotarod test (D, E) and open-field test (F, G) were used to evaluate the motor function of the PD mice. Compared with the control group, the group that received a 10  $\mu$ g 6-OHDA injection exhibited decreased use of the left forelimb in the cylinder test, decreased speed and latency in the rotarod test, and decreased rearing frequency in the open field test ( $P < .01$ ). NAD (20  $\mu$ g) increased the use of the left forelimb in the cylinder test and the speed in the rotarod test ( $P < .05$ ), and increased the latency in the rotarod test with a borderline significance. No significant differences were observed in the open field test after NAD preadministration.  $N = 11-15$ , \* $P < .05$ , \*\* $P < .01$ , \*\*\* $P < .001$ .

157 ectoenzymes, which function together with NAD to regulate the mitigation of many age-related diseases in murine models (Imai et al., 2014). Studies have demonstrated that NAD restoration by the administration of key NAD intermediates/precursors, such as nicotinamide mononucleotide (NMN) and nicotinamide riboside (NR), can dramatically alleviate the age-associated functional defects of some neurodegenerative diseases (Pehar et al., 2018). For instance, dietary NR supplementation has been reported to benefit cognition and synaptic plasticity in a transgenic mouse model of Alzheimer's disease, in part by promoting  $\beta$ -secretase ubiquitination and degradation (Gong et al., 2013). What is more intriguing is that chronic NR replenishment is found to be well tolerated and can effectively elevate NAD levels in the peripheral blood mononuclear cells (PBMCs) of healthy middle-aged and older adults (Martens et al., 2018), indicating the translational potential of NAD in treating neurodegenerative diseases. However, whether NAD restoration can play a beneficial role in PD is not clear.

Sirtuins, which are highly conserved NAD<sup>+</sup>-dependent enzymes, are key modulators of many important biological pathways, such as inflammatory reactions, the stress response and protein aggregation, which are closely related to age-related neurodegenerative diseases (Donmez, 2012). There are seven human homologs of the sirtuin family (SIRT1–7) that have distinct subcellular localizations and thus serve a diverse array of biological functions (Michishita et al., 2005). In the context of PD, SIRT1 and SIRT2 are the most common sirtuins studied thus far (Donmez, 2012). Sirt1 is predominantly expressed in neurons and is located in the nucleus. It has been reported to protect neurons from neurotoxicity induced by  $\alpha$ -synuclein, which is the main histopathological component of PD (Peelaerts et al., 2016), by activating peroxisome proliferator-activated receptor gamma coactivator 1 $\alpha$  (PGC1 $\alpha$ ) (Wareski et al., 2009). Sirt2, a cytoplasmic protein, can enhance dopaminergic differentiation via the AKT/GSK-3 $\beta$ / $\beta$ -catenin pathway (Szego et al., 2017). The inhibition of Sirt2 rescues the  $\alpha$ -

synuclein-induced toxicity of dorsomedial dopamine neurons and modifies  $\alpha$ -synuclein aggregation in PD models (Outeiro et al., 2007). Few studies have highlighted the potential roles of other sirtuins in PD pathology.

To test the hypothesis that NAD exerts protective effects in PD, we investigated whether an intra-ST injection of NAD can ameliorate the behavioral deficits and reduce dopaminergic neuronal damage in a 6-hydroxydopamine (6-OHDA)-induced mouse model of PD and whether NAD can counteract the mitochondrial defects and oxidative stress induced by 6-OHDA in vitro. As sirtuins are NAD<sup>+</sup>-dependent enzymes that have beneficial effects against age-related diseases, we also explored whether the protective function of NAD on dopaminergic neurons is mediated by signaling pathways related to sirtuins.

## 2. Materials and methods

### 2.1. Animals and surgical procedure

All animal experiments in this study were approved by the ethics committee of Shanghai Jiao Tong University (SJTU) and conducted according to the National Institutes of Health Guidelines for the Care and Use of Laboratory Animals (NIH Publications No. 8023, revised 1978). C57BL/6 male mice (25–30 g) were purchased from SLACCAS Laboratory Animal Company (Shanghai, China) and housed under a 12-h light/dark cycle at the Laboratory Animal Center of SJTU with free access to food and water.

Eighty mice were randomly assigned to four groups: the control group, the control + NAD (20  $\mu$ g) group, the 6-OHDA (10  $\mu$ g) group and the 6-OHDA (10  $\mu$ g) + NAD (20  $\mu$ g) group. The mice in the control group received the normal saline (N.S.) and 0.02% (w/v) VitC in the right ST. N.S. was used as the solvent of NAD, and 0.02% (w/v) VitC in N.S. was used as the solvent of 6-OHDA to prevent its autooxidation. Seven mice died after the surgery. Twenty mice were sacrificed for the immunostaining 1 week after the surgery and the other 53 mice received the behavioral tests 4 weeks after the surgery. A model of PD was established by an injection of 6-OHDA into the right ST; this procedure is commonly used to establish rodent models of PD (Przedborski et al., 1995) and has been confirmed in our published studies to cause dopaminergic neuronal loss in both the SN and ST (Guo et al., 2017; Guo et al., 2018). In brief, the mice were first anesthetized with 1% pentobarbital sodium (0.8 ml/kg) and then placed in a stereotaxic apparatus. After the scalp was incised at the midline, a tiny hole was drilled, and 10  $\mu$ g 6-OHDA (5  $\mu$ g/ $\mu$ l in 2  $\mu$ l) was injected into the right ST at a rate of 1  $\mu$ l/min using a 10  $\mu$ l syringe (Hamilton) according to the following coordinates: AP: 0.5 mm, ML: 2 mm, and DV: - 3.3 mm. The mice were intraperitoneally injected with 25 mg/kg desipramine 30 min before the injection of 6-OHDA to prevent damage to noradrenergic neurons, and the needle was left for another 10 min and withdrawn slowly to reduce reflux along the needle track. Finally, the skin was closed and routinely disinfected. Twenty micrograms of NAD (10  $\mu$ g/ $\mu$ l in 2  $\mu$ l) was injected at the same coordinates 4 h before the injection of 6-OHDA. The schedule of the animal experiments is presented in Fig. 1A.

### 2.2. Apomorphine-induced rotation test

The apomorphine-induced rotation test was conducted as previously described in 6-OHDA-lesioned rats (Przedborski et al., 1995) to evaluate the functional alteration of dopaminergic neurons in the nigrostriatal system of the 6-OHDA injected mice. The mice were allowed to habituate for 10 min in a white 27.5  $\times$  27.5 cm chamber. Immediately after the intraperitoneal injection of 0.5 mg/kg apomorphine hydrochloride, full rotations in the chamber were recorded with a video camera for 30 min and counted by a blinded examiner.

### 2.3. Behavioral tests

#### 2.3.1. Open field test (OFT)

We performed the OFT in this study to evaluate the motor activity of the 6-OHDA- and/or NAD-treated mice. The mice were placed into the central area of the OFT chamber (a white 27.5  $\times$  27.5 cm chamber with an open top) and allowed to explore freely for 5 min. All activities inside the chamber were monitored by a video camera and tracked using the ANY-maze automated video system (Version 4.115; Stoelting Co., Wood Dale, IL, USA). The movement distance and rearing frequency were analyzed to evaluate motor function and the exploration activity of the mice.

#### 2.3.2. Cylinder test (CT)

The CT was utilized to reflect the motor asymmetry of the mice, as unilateral 6-OHDA-induced lesions in the right ST cause motor dysfunction of the ipsilateral (left) limbs (Schallert et al., 2000). Each mouse was placed into a transparent cylinder (25 cm in diameter, 60 cm high) for 3 min, and the frequency with which the left forelimb, the right forelimb, and both forelimbs were used during rearing was recorded by a blinded examiner. The data are presented as the frequency ratio of left/right forelimb wall touches.

#### 2.3.3. Rotarod test

The rotarod test was used to evaluate the motor coordination of the mice (Rozas et al., 1998). A rotarod system with 5 individual chambers was used in this study. Over the course of 5 min, the rotation speed of the rod gradually increased from 4 to 40 rpm, and the mice were forced to run forward on the motorized rod (30 mm in diameter). Once a mouse was unable to keep up with the increasing speed and fell off the rod, the rotation speed and time latency were recorded. Five trials were repeated to calculate the average speed and latency achieved by the mice.

### 2.4. Western blot

Mouse brain tissues or cells were lysed in RIPA supplemented with 1  $\times$  protease and phosphatase inhibitor cocktail and then centrifuged to collect the supernatant. The total protein concentration was quantified using BCA protein assay reagents, and 20  $\mu$ g protein was run on an SDS-PAGE gel and transferred to a PVDF membrane. The membranes were blocked with 5% nonfat milk in 0.1% TBST for 2 h at room temperature and then incubated with a primary antibody overnight at 4  $^{\circ}$ C. After incubation with HRP-conjugated secondary antibodies for 2 h at room temperature, the blots were developed with an ECL reagent. The primary antibodies used in this study are as follows: anti-TH (1: 5000), anti-Sirt1 (1: 1000), anti-Sirt2 (1: 1000), anti-Sirt3 (1: 1000), anti-acetyl-p53 (1: 1000), anti-p53 (1: 1000), anti-acetyl-SOD2 (1: 1000), anti-SOD2 (1: 1000), anti-PARP (1: 1000), anti-COX2 (1: 1000), anti-ND1 (1: 1000), anti-ATP6 (1: 1000), anti-GAPDH (1: 5000), and anti-beta-actin (1: 5000).

### 2.5. Immunohistochemistry

One week after 6-OHDA-injection, 5 mice per group were deeply anesthetized with 1% pentobarbital sodium (0.8 ml/kg), perfused transcardially with 0.1 M PBS and fixed with 4% paraformaldehyde (PFA). The brains were dissected, postfixed, dehydrated, embedded in paraffin and sectioned at a thickness of 4  $\mu$ m. Every fifth section containing the SN or ST was collected, and 5 sections per sample were subjected to immunostaining. Briefly, after endogenous peroxidase activity was inactivated by 3% H<sub>2</sub>O<sub>2</sub> and the antigen was retrieved by citric acid buffer, the sections were blocked with 5% goat serum and incubated with a primary antibody against tyrosine hydroxylase (TH, 1: 400) overnight at 4  $^{\circ}$ C. On the second day, the sections were incubated with a biotin-conjugated goat anti-rabbit IgG secondary antibody, and

staining was performed using the avidin-biotin complex (ABC) system and nickel-enhanced diaminobenzidine (DAB) incubation (Vectastain Elite, Vector Labs, Burlingame, CA). Images were obtained using a microscope (Olympus IX70, Japan). The number of TH-positive neurons in the SN and the fractions of TH-positive area in the ST were measured using ImageJ 1.49v (National Institutes of Health, USA). The data are expressed as a percentage of the TH-positive neuron number or area fraction on the impaired side relative to that on the intact side.

## 2.6. Cell culture and viability

The rat pheochromocytoma PC12 cell line was used in this study to explore the protective role of NAD against the neurotoxicity of 6-OHDA in vitro. PC12 cells were cultured in Dulbecco's modified Eagle's medium (DMEM) supplemented with 10% horse serum, 5% fetal bovine serum and 1% penicillin/streptomycin. The cells were grown in a 5% CO<sub>2</sub> humidified atmosphere at 37 °C, and the medium was replaced every 2–3 days.

The effects of NAD and 6-OHDA on PC12 cell viability were evaluated using a Cell Counting Kit-8 (CCK-8), which determines cell viability by utilizing a highly water-soluble tetrazolium salt that produces a water-soluble formazan dye upon reduction in the presence of the dehydrogenase in living cells, according to the manufacturer's protocol and as previously described (Guo et al., 2018). Briefly, the PC12 cells were seeded in a 96-well plate at a density of  $5 \times 10^3$  cells per well. NAD (10 μM, 50 μM and 200 μM) was administered 2 h before the application of 200 μM 6-OHDA, and then the cells were incubated for 24 h. The CCK-8 (10 μl) solution was added to each well, and the cells were incubated for 1 h at 37 °C. Finally, the optical absorbance was measured at 450 nm using a microplate reader. The data were normalized to that of the controls.

To exclude the possibility that NAD reacts directly with 6-OHDA, we monitored the formation of p-quinone and thiol conjugates, which result from the autooxidation of 6-OHDA, at 350 nm and 490 nm, respectively, with a microplate reader, as previously described (Soto-Otero et al., 2000). All in vitro assays were performed in triplicate, and each experiment was repeated three times independently.

## 2.7. Quantitative determination of NAD<sup>+</sup>

The quantitative determination of NAD<sup>+</sup> was performed using an EnzyChrom™ NAD<sup>+</sup>/NADH Assay Kit (E2ND-100, Bioassay Systems), which is based on a lactate dehydrogenase reaction cycle in which NADH is formed and reduces the formazan (MTT) reagent, according to the manufacturer's protocol and as previously described (Bai et al., 2011). The colour intensity of the reduced product, which can be measured at 565 nm, is proportional to the NAD<sup>+</sup>/NADH concentration. Briefly,  $\sim 10^6$  PC12 cells were homogenized with 100 μl of NAD extraction buffer and then heated at 60 °C for 5 min. Next, 20 μl of assay buffer and 100 μl of NADH extraction buffer were successively added to neutralize the extracts, and then the samples were centrifuged at 14,000 rpm for 5 min to collect the supernatant for the NAD assay. The working reagent was prepared by mixing 60 μl of assay buffer, 1 μl of enzyme A, 1 μl of enzyme B, 14 μl of lactate and 14 μl of MTT. Then, 40 μl of each sample and 80 μl of the working reagent were added to a transparent flat-bottom 96-well plate. The optical density was read at 565 nm at time zero and at 15 min, which was after a 15-min incubation period.

## 2.8. Reactive oxygen species (ROS) detection

H2DCFDA, a cell-permeable fluorogenic probe that can be modified by cellular esterases to form a nonfluorescent H2DCF, was used for ROS detection in this study. The oxidation of H2DCF by intercellular ROS yields a fluorescent product whose intensity is proportional to the ROS levels. According to the manufacturer's protocol of the ROS Detection

Assay Kit (K936–100, Biovision),  $5 \times 10^4$  PC12 cells were plated in each well of a 96-well plate and were washed in 100 μl of ROS assay buffer and then incubated with 100 μl of  $1 \times$  ROS label diluted in ROS assay buffer for 45 min at 37 °C in the dark. Later, the ROS label was removed, and 100 μl of ROS assay buffer was added to each well. The fluorescence at Ex/Em 495/529 nm in end point mode was measured immediately.

## 2.9. Superoxide dismutase (SOD) detection

We used the SOD assay kit-WST (S311, Dojindo) to measure SOD levels by utilizing WST-1, a highly water-soluble tetrazolium salt that produces a water-soluble formazan dye upon reduction by superoxide anion, which can be inhibited by SOD. Approximately  $10^6$  cells were lysed in 100 μl of RIPA supplemented with  $1 \times$  protease and phosphatase inhibitor cocktail and then centrifuged to collect the supernatant. A WST working solution (1 ml of WST solution diluted in 19 ml of buffer solution) and an enzyme working solution (15 μl of mixed enzyme solution diluted in 2.5 ml of dilution buffer) were later prepared, and then 20 μl of sample solution was added to each sample and blank 2 well, while 20 μl of ddH<sub>2</sub>O was added to each blank 1 and 3 well. Then, 200 μl of WST working solution was pipetted into each well. Successively, 20 μl of dilution buffer was added to each blank 2 and 3 well, while 20 μl of enzyme working solution was added to each sample and blank 1 well. After mixing thoroughly, the plate was incubated at 37 °C for 20 min, and the absorbance was read at 450 nm using a microplate reader. SOD activity was calculated as  $[(A_{\text{blank1}} - A_{\text{blank3}}) - (A_{\text{sample}} - A_{\text{blank2}})] / (A_{\text{blank1}} - A_{\text{blank3}}) \times 100\%$ .

## 2.10. Gene expression analysis by quantitative PCR

The cells were lysed thoroughly in Taq Plus Master Mix to extract the total cellular DNA, which was later evaluated with a Nano Bioanalyzer and used in PCR amplification. Quantitative PCR was performed on a LightCycler 480 Real-Time PCR System (Roche) using the following primers: ATP synthase subunit 6 (ATP6) (forward: TAG CCATCCCCCTATGAGCA and reverse: TTCCTTGCGGTGAGAAGTGG), NADH dehydrogenase subunit 1 (ND1) (forward: CCCATACGCCCTCT AACCAC and reverse: TAAGGGGGTGGGGTATTGGT), cytochrome c oxidase subunit 2 (COX2) (forward: TGTTCATTGTGAAGATTCTCT GTG, and reverse: GCCGGTATCTGCCTTCATGT), TRPM1 (forward: AGACGGGTGAGACAGCTGCACCTTTTC and reverse: CGAGAGCATCA AGTGCAGGATTAGAG), and GAPDH (forward: AGAATGGATGCCTG TGTTGGG and reverse: CTTCCCATCACCCCTAAGCC).

## 2.11. Isolation of mitochondria

PC12 cell pellets were collected and washed 3 times in prechilled 0.1 M PBS. Then, the mitochondria were isolated following the general differential centrifugation method described by Frezza et al. with minor modifications (Frezza et al., 2007). Briefly, the washed PC12 cell pellet was resuspended in 1 ml of mitochondrial isolation buffer and homogenized with 30 strokes of a teflon Teflon pestle in a prechilled glass mortar. The homogenate was centrifuged at  $600 \times g$  for 10 min at 4 °C. The supernatant was collected and then centrifuged at  $11,000 \times g$  for 10 min at 4 °C. The supernatant was discarded, and the mitochondrial pellet was collected.

## 2.12. Detection of mitochondrial parameters

MitoTracker Green (C1048, Beyotime) was used for the quantification of mitochondrial content as previously described (Peng et al., 2017). Briefly, 50 μg MitoTracker Green was dissolved in 74.4 μl of DMSO to make a 1 mM stock solution. Then,  $\sim 10^6$  PC12 cells were washed in PBS and incubated in a 200 nM MitoTracker working solution (diluted in DMEM at 1: 5000 and preincubated at 37 °C) at 37 °C for

30 min. The fluorescence was observed by an inverted fluorescence microscope. In addition, to detect the mitochondrial membrane potential (MMP), a JC-1 working solution was first made by diluting 50  $\mu$ l of JC-1 (200 $\times$ , C2006, Beyotime) with 8 ml of ultrapure water and 2 ml of JC-1 buffer (5 $\times$ ) to make a final concentration of 5  $\mu$ g/ml. Approximately  $10^6$  cells were incubated in 1 ml of JC-1 working solution at 37 °C for 20 min and then washed two times in JC-1 buffer. JC-1 accumulates in the mitochondrial matrix and forms J-aggregates that fluoresce red when the MMP is normal; however, when the MMP is lower, JC-1 cannot accumulate in the mitochondrial matrix and thus is present as a monomer, which fluoresces green. The ratio of green/red fluorescence reflects mitochondrial depolarization (Zhu et al., 2009). Tetramethylrhodamine methyl ester perchlorate (TMRM, Sigma T5428) was also used to verify the effect of NAD on the MMP. Briefly, 25 mg TMRM was dissolved in 5 ml of DMSO to make a 10 mM stock solution, which was further diluted with DMSO to reach a concentration of 10  $\mu$ M. PC12 cells were loaded with 100 nM TMRM for 30 min at 37 °C and then the fluorescence was observed by an inverted fluorescence microscope.

ATP levels, which is another parameter that reflects mitochondrial function, was measured by an ATP Colorimetric Assay Kit (K354–100, Biovision), which utilizes the phosphorylation of glycerol to generate a product that is easily quantified by colorimetric analysis (OD 570 nm), as previously described (Wu et al., 2017). According to the manufacturer's protocol,  $1 \times 10^6$  cells were lysed with 100  $\mu$ l ATP assay buffer, and 50  $\mu$ l of the lysed supernatant was used for the following assay. First, 50  $\mu$ l of each samples was added to a 96-well plate, and then a total of 50  $\mu$ l of reaction mix, which included 44  $\mu$ l of ATP assay buffer, 2  $\mu$ l of ATP probe, 2  $\mu$ l of ATP converter and 2  $\mu$ l of developer, was added to each well. The wells were mixed and incubated at room temperature for 30 min. The absorbance at OD 570 nm was measured with a microplate reader.

### 2.13. Materials

$\beta$ -Nicotinamide adenine dinucleotide (N0632), 6-hydroxydopamine hydrobromide (H116), desipramine hydrochloride, RIPA and TMRM (T5428) were purchased from Sigma (St. Louis, MO). The protease and phosphatase inhibitor cocktail, and BCA protein assay reagents were obtained from Thermo Fisher Scientific (Fair Lawn, NJ, USA). The ABC and DAB kits were purchased from Vector Laboratories, Inc. (Burlingame, CA).

DMEM, heat-inactivated endotoxin-free fetal bovine serum and horse serum were obtained from Gibco (Logan, UT). The CCK-8 assay and the SOD Assay Kit-WST (S311) were from Dojindo. The EnzyChrom™ NAD<sup>+</sup>/NADH Assay Kit (E2ND-100) was purchased from Bioassay Systems. The ATP Colorimetric Assay Kit (K354–100) and the ROS Detection Assay Kit (K936–100) were obtained from Biovision. MitoTracker Green (C1048), the JC-1 Assay Kit (C2006) and Hoechst 33342 (C1028) were purchased from Beyotime Biotechnology (Wuhan, China). The Antibody against TH was from Millipore (Cambridge, MA, USA). The antibodies against Sirt1, Sirt2, Sirt3, p53, and acetyl-SOD2 as well as all secondary antibodies, were obtained from Cell Signaling Technology (Beverly, MA). The antibody against acetyl-p53 was obtained from Abcam (Cambridge, UK) and the antibodies against SOD2, ND1, MTCO2 and ATP6 were obtained from Proteintech (Rosemont, IL, USA). Taq Plus Master Mix (P211) and SYBR (Q511) were obtained from Vazyme (Nanjing, China).

### 2.14. Statistical analysis

The statistical analysis used in this study was one-way ANOVA followed by post hoc comparisons using Tukey's test or Dunnett's T3 test for comparisons among multiple groups, and the data were analyzed with SPSS 24.0 (IBM, Armonk, NY, USA). In order to reduce the impact of accidental factors and individual differences on the test results, the

data from our behavioral tests were normalized to the averages of the mice in the control group from each cohort because we conducted the behavioral experiments in two cohorts. All data are presented as the mean  $\pm$  SEM.  $P < .05$  was considered statistically significant.

## 3. Results

### 3.1. NAD preadministration ameliorated motor deficits in PD mice

Four weeks after 6-OHDA lesion, apomorphine-induced rotation was evaluated. It was demonstrated that the 6-OHDA-injected mice exhibited dramatic rotation toward the left side compared with control mice ( $t = 13.87$ ,  $df = 25$ ,  $P < .001$ , Fig. 1B), indicating the successful unilateral depletion of nigrostriatal dopaminergic innervation induced by 6-OHDA.

The animals were then subjected to various tests of motor function, including the CT, the rotarod test and the OFT, to detect behavioral dysfunction. When subjected to the CT, the 6-OHDA-injected mice showed a significant defect in the frequency of left forelimb touches compared with that of the controls ( $F_{(3, 49)} = 14.88$ ,  $P < .001$ , post hoc: control vs 6-OHDA,  $P < .001$ ), but this defect was significantly improved by preinfusion with NAD ( $P < .001$ , Fig. 1C). The rotarod test was used to assess the coordination and balance of the mice. 6-OHDA lesions resulted in a markedly decreased normalized speed ( $F_{(3, 49)} = 6.409$ ,  $P < .001$ , post hoc: control vs 6-OHDA,  $P < .001$ ) and normalized latency ( $F_{(3, 49)} = 5.411$ ,  $P = .0027$ , post hoc: control vs 6-OHDA,  $P = .002$ ) in the rotarod test, but the preadministration of NAD effectively ameliorated this motor deficit ( $P < .05$ , Fig. 1D;  $P = .05$ , Fig. 1E). In the OFT, there was a significant decrease in normalized rearing frequency ( $F_{(3, 49)} = 10.99$ ,  $P < .001$ , post hoc: control vs 6-OHDA,  $P < .001$ ) and a tendency for the normalized movement distance of 6-OHDA-lesioned mice to decrease ( $F_{(3, 49)} = 5.175$ ,  $P = .0038$ , post hoc: control vs 6-OHDA,  $P = .157$ ), while no improvement in this abnormality was found with treatment with NAD ( $P > .05$ , Fig. 1F, G). All detailed data for the behavioral tests are presented in Supplementary Table 1.

### 3.2. NAD prevented dopaminergic neuronal loss in the SN and ST

Because dopaminergic neuronal loss in the nigrostriatal system is the main pathological event in PD, we determined whether NAD can exert a protective effect on dopaminergic neurodegeneration in the SN and ST of PD mice.

The results from TH immunostaining in the SN showed that nearly 50% of the TH-positive neuronal loss was observed on the right side compared with the left side in the 6-OHDA-lesioned mice ( $F_{(3, 16)} = 12.97$ ,  $P < .001$ , post hoc: control vs 6-OHDA =  $1.000 \pm 0.074$  vs  $0.508 \pm 0.069$ ,  $n = 5$ ,  $P < .001$ ), whereas preinjection with NAD significantly reduced the loss of the TH-positive neuron in the SN (6-OHDA vs 6-OHDA + NAD =  $0.508 \pm 0.069$  vs  $0.777 \pm 0.040$ ,  $n = 5$ ,  $P = .037$ , Fig. 2A, B).

In agreement with this observation, a decrease of the TH-positive fibers in the ST was also found in the 6-OHDA-lesioned mice as determined by immunohistochemical staining ( $F_{(3, 16)} = 63.95$ ,  $P < .001$ , post hoc: control vs 6-OHDA =  $1.000 \pm 0.044$  vs  $0.278 \pm 0.038$ ,  $n = 5$ ,  $P < .001$ ), and this decrease was reversed by NAD intervention (6-OHDA + NAD =  $0.278 \pm 0.038$  vs  $0.554 \pm 0.066$ ,  $n = 5$ ,  $P = .002$ , Fig. 2C, D). Western blotting confirmed the neuroprotective effect of NAD on the expression of TH in the ST (Fig. 2E).

### 3.3. NAD alleviated 6-OHDA-induced oxidative stress and mitochondrial dysfunction in PC12 cells

To investigate how NAD protects against dopaminergic neurodegeneration, PC12 cells were used to identify the related molecular

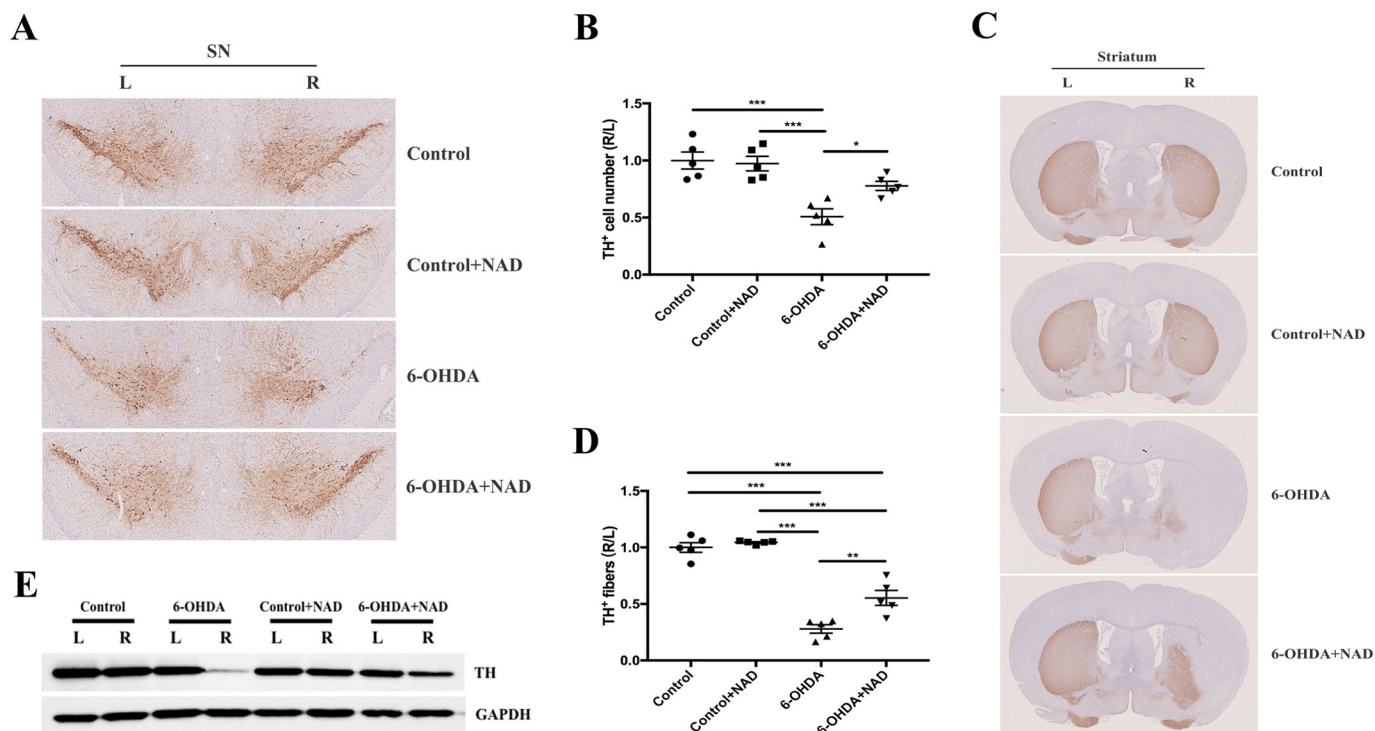


**Fig. 2.** NAD prevented dopaminergic neuronal loss in the SN and ST of PD mice. 6-OHDA (10  $\mu$ g) induced ~ 50% dopaminergic neuronal loss in the right SN compared to the left SN, and this loss was improved by preinjection with 20  $\mu$ g NAD (A, B). Similarly, 6-OHDA induced ~ 72.2% dopaminergic fiber loss in the ST on the lesioned side compared to the intact side, and this loss was improved by preinjection with NAD (C, D). The results of western blotting of ST tissue were in line with the immunohistochemical results (E).  $N = 5$ , \* $P < .05$ , \*\* $P < .01$ , \*\*\* $P < .001$ .

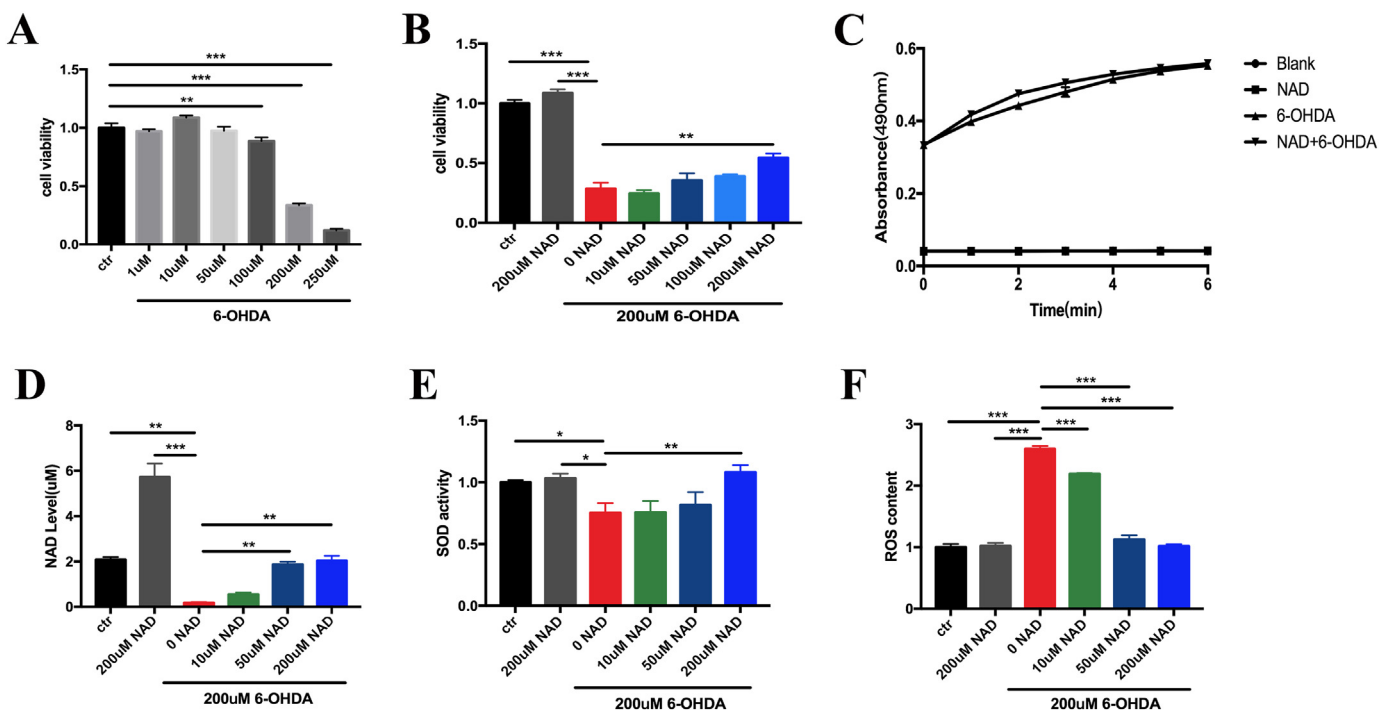


**Fig. 3.** NAD protected PC12 cells against 6-OHDA-induced loss of cell viability and oxidative stress. Cell viability was measured by CCK-8 after the PC12 cells were incubated with various concentrations of 6-OHDA for 24 h (A). The pretreatment of the PC12 cells with various concentrations of NAD was performed 2 h before exposure to 200  $\mu$ M 6-OHDA, and the rescue of cell viability induced by NAD was detected at 24 h (B). The effects of NAD on the auto-oxidation of 6-OHDA were measured spectrophotometrically at 490 nm using a microplate reader (C). NAD (10  $\mu$ M, 50  $\mu$ M or 200  $\mu$ M) was applied 2 h before 200  $\mu$ M 6-OHDA, and the NAD level (D), SOD activity (E) and ROS levels (F) were measured 2 h after 6-OHDA treatment. 6-OHDA caused a significant decrease in the NAD level and SOD activity as well as an obvious increase in ROS levels, while NAD pretreatment reversed this phenomenon to some extent. The values were obtained from three independent experiments. \* $P < .05$ , \*\* $P < .01$ , \*\*\* $P < .001$ .

mechanism. As shown in Fig. 3A, 24 h of exposure to 6-OHDA resulted in a dose-dependent decrease in cell viability ( $F_{(6, 14)} = 616.1$ ,  $P < .001$ ), with a concentration of 200  $\mu\text{M}$  causing nearly 50% toxicity ( $P < .001$ ). This concentration (200  $\mu\text{M}$ ) was used in all subsequent experiments. The preincubation of the PC12 cells with 200  $\mu\text{M}$  NAD markedly reduced the 6-OHDA-induced reduction in cell viability ( $F_{(6, 14)} = 81.46$ ,  $P < .001$ , post hoc: 6-OHDA vs 6-OHDA + 200  $\mu\text{M}$  NAD,  $P = .0042$ , Fig. 3B). Moreover, the PC12 cells lost their normal cellular morphology and detached from the bottom of the culture dish after incubation with 200  $\mu\text{M}$  6-OHDA for 24 h, while pretreatment with NAD dramatically alleviated the morphological injuries in a dose-dependent manner (Supplementary Fig. 1). To exclude the possibility that NAD may react directly with 6-OHDA, we monitored the autoxidation products of 6-OHDA incubated with NAD by a spectrophotometric assay and found no difference with those of 6-OHDA itself (Fig. 3C).

To explore why preincubation with NAD exerts a protective role against 6-OHDA toxicity in PC12 cells, we measured whether 6-OHDA leads to NAD exhaustion. 6-OHDA (200  $\mu\text{M}$ ) caused a marked decrease in the NAD level in PC12 cells ( $F_{(5, 12)} = 52.99$ ,  $P < .001$ , post hoc: Ctr vs 6-OHDA,  $P = .0032$ ), while supplementation with 50  $\mu\text{M}$  and 200  $\mu\text{M}$  NAD effectively helped to maintain NAD levels ( $P = .0081$  and  $P = .0039$ , respectively, Fig. 3D). As increased oxidative stress is one of the prominent features of PD, we measured the activity of two important indicators of oxidative stress, SOD and ROS. 6-OHDA caused decreased SOD activity ( $F_{(5, 12)} = 4.22$ ,  $P = .019$ ) and increased ROS release ( $F_{(5, 12)} = 224.3$ ,  $P < .001$ ) in the PC12 cells, and these changes were significantly reversed by NAD in a dose-dependent manner ( $P < .05$ , Fig. 3E, F).

Mitochondrial dysfunction and subsequent cellular energy failure and oxidative stress, may be important mechanisms in PD pathophysiology (Kruger et al., 2017). Therefore, we further evaluated mitochondrial function alterations after 6-OHDA and NAD administration. We first conducted MitoTracker fluorescent staining to quantify the mitochondria. The results showed an obvious reduction in green fluorescence intensity in the 6-OHDA group compared with the control ( $F_{(5, 28)} = 23.48$ ,  $P < .001$ , post hoc: control vs 6-OHDA,  $P < .001$ ), which was significantly improved with the preadministration of 10  $\mu\text{M}$ , 50  $\mu\text{M}$  or 200  $\mu\text{M}$  NAD ( $P < .05$ , Fig. 4A, B). In addition, mitochondrial bioenergetic function was also evaluated in the current study. When ATP levels were evaluated, the 6-OHDA-induced decrease in the ATP level was found to be alleviated by 200  $\mu\text{M}$  NAD ( $F_{(5, 12)} = 141.8$ ,  $P < .001$ , post hoc: 6-OHDA vs 6-OHDA + 200  $\mu\text{M}$  NAD,  $P < .001$ , Fig. 4C). In addition, q-PCR and western blotting were used to detect the expression of mitochondrial bioenergetic markers, including ATP6, ND1 and COX2. There was a marked increase in the copy numbers of mitochondrial bioenergetic markers in the PC12 cells after incubation with 6-OHDA for 24 h; compared to the control group, the 6-OHDA group exhibited a relative expression of ATP6 that was 145.4 times higher ( $F_{(5, 12)} = 64.46$ ,  $P < .001$ , post hoc: control vs 6-OHDA,  $P < .001$ ), a relative expression of ND1 that was 187.2 times higher ( $F_{(5, 12)} = 35.61$ ,  $P < .001$ , post hoc: control vs 6-OHDA,  $P = .0152$ ) and a relative expression of COX2 that was 2.906 times higher ( $F_{(5, 12)} = 6.944$ ,  $P = .0029$ , post hoc: control vs 6-OHDA,  $P = .0104$ ). Pretreatment with 10  $\mu\text{M}$ , 50  $\mu\text{M}$  or 200  $\mu\text{M}$  NAD significantly reduced this increase in mitochondrial expression at the mRNA level ( $P < .05$ , Fig. 4D, E, F). Similarly, increased protein expressions of ATP6, ND1, and COX2 were observed following 6-OHDA exposure, and this increase was reversed by preincubation with NAD (Fig. 4G).

JC-1 and TMRM staining were then utilized to detect cellular MMP. As expected, the red/green fluorescence intensity decreased in the 6-OHDA group when stained with JC-1, and this ratio was markedly increased by preincubation with 200  $\mu\text{M}$  NAD ( $F_{(5, 21)} = 11.24$ ,  $P < .001$ , post hoc: 6-OHDA vs 6-OHDA + 200  $\mu\text{M}$  NAD,  $P = .001$ , Fig. 5A, B). Similarly, the 6-OHDA-induced decrease in red fluorescence intensity in the mitochondria was reversed by preincubation with 200  $\mu\text{M}$  NAD in the TMRM immunostaining ( $F_{(5, 21)} = 9.638$ ,  $P < .001$ ,

post hoc: 6-OHDA vs 6-OHDA + 200  $\mu\text{M}$  NAD,  $P = .02$ , Fig. 5C, D).

Sirtuins have been reported to mediate the regulation of metabolic homeostasis by NAD and longevity in worms and mice (Mouchiroud et al., 2013; Fang et al., 2016); thus, we further explored whether NAD protects PC12 cells against 6-OHDA toxicity via sirtuin signaling. The cells were administered various concentrations of 6-OHDA, and we observed a significant decrease in Sirt3 with 200  $\mu\text{M}$  6-OHDA ( $F_{(5, 12)} = 6.273$ ,  $P = .004$ , post hoc: control vs 200  $\mu\text{M}$  6-OHDA,  $P = .002$ , Fig. 6A, B). 6-OHDA (200  $\mu\text{M}$ ) also caused a time-dependent change in the expression of Sirt3 ( $F_{(5, 12)} = 17.247$ ,  $P < .001$ ), but not of Sirt1 or Sirt2 ( $P > .05$ , Fig. 6C, D). Moreover, pretreatment with different concentrations of NAD reduced the 200  $\mu\text{M}$  6-OHDA-induced decreased expression of Sirt3 in a dose-dependent manner, no matter in total protein ( $F_{(5, 18)} = 8.256$ ,  $P < .001$ ) or mitochondrial protein ( $F_{(5, 18)} = 9.751$ ,  $P < .001$ , Fig. 6E, F, G, H). The in vivo results confirmed this phenomenon, that is, 10  $\mu\text{g}$  6-OHDA led to an 18.1% lower expression of Sirt3 in the right ST compared with the left ST ( $P = .048$ ), while the preinjection of 20  $\mu\text{g}$  NAD prevented this decrease with borderline significance ( $P = .071$ , Fig. 6I, J). However, no obvious alterations were found in the expression of the Sirt3-targeted genes SOD2 and p53 ( $P > .05$ , Fig. 6E, G, I).

#### 4. Discussion

In the current study, we demonstrated that the preadministration of NAD can ameliorate motor deficits and dopaminergic neuronal loss in the nigrostriatal system of 6-OHDA-lesioned PD mice. In addition, the in vitro results showed that NAD protects PC12 cells against the 6-OHDA-induced loss of cell viability, morphological damage, oxidative stress and mitochondrial dysfunction.

Mounting evidence has demonstrated a correlation between compromised NAD<sup>+</sup> status with aging and neurodegeneration. In particular, in vivo imaging data has shown for the first time that NAD<sup>+</sup> levels decline in the brains of healthy aged humans compared to younger subjects (Zhu et al., 2015). In addition, decreased levels of NAD<sup>+</sup> have been reported in vivo in a Drosophila model of PD with a parkin mutation (Lehmann et al., 2016) and in vitro in the rotenone-treated PC12 cells (Lu et al., 2014), Fbxo7-knockdown SH-SY5Y cells (Delgado-Camprubi et al., 2017) and induced pluripotent stem cell (iPSC)-derived neurons from PD patients bearing mutations in the  $\beta$ -glucocerebrosidase (GBA) gene (Schondorf et al., 2018). In line with this, our in vitro results also demonstrated a depletion of NAD when 6-OHDA was applied to PC12 cells. Although recent studies in rotenone-treated PC12 cells and Drosophila models of PD with pink1 mutations have shown that NAD<sup>+</sup> supplementation can ameliorate PD phenotypes (Lu et al., 2014; Lehmann et al., 2017), studies of NAD<sup>+</sup> restoration in PD mice are still needed to elucidate the underlying beneficial roles of NAD<sup>+</sup> in PD pathology (Fang et al., 2017).

In our study, we observed that preadministration with 20  $\mu\text{g}$  NAD can effectively ameliorate motor dysfunction in 6-OHDA-induced PD mice, as evaluated by the cylinder test and rotarod test; however, we failed to find a significant improvement in the distance traveled and rearing frequency in the OFT after NAD treatment. As the OFT reveals a complex pattern of both movement and emotion (Walsh et al., 1976), emotion-related factors such as anxiety or depression may contribute to the inconsistency with the results of the other two tests of motor behavior. In addition to improving motor dysfunction in the 6-OHDA-induced PD mice, NAD replenishment was also found to attenuate dopaminergic neuronal death in both the SN and ST in the current study, which is the typical pathological characteristic of PD. This finding may also explain why NAD can ameliorate motor dysfunction in PD mice. All the results indicate that NAD may have the translational potential to both relieve symptoms and treat the etiology of PD.

At present, the results whether there is an apoptotic change in the SN after 6-OHDA injection were controversial. Although apoptosis has been observed in the SN following 6-OHDA-induced lesion in some

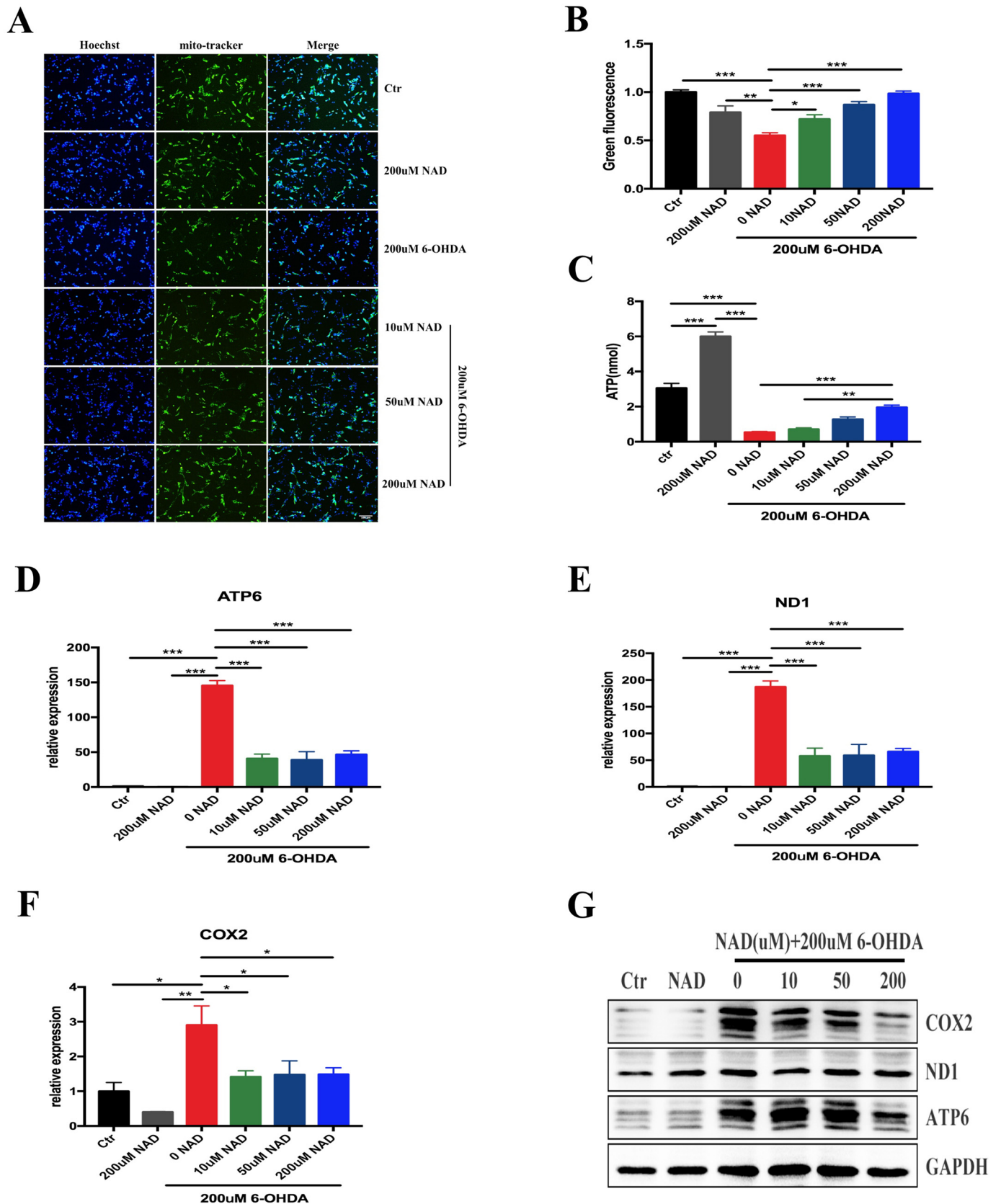


**Fig. 4.** NAD alleviated 6-OHDA-induced mitochondrial dysfunction in PC12 cells. MitoTracker Green was used to stain the mitochondria (A, B) 2 h after 200 µM 6-OHDA incubation. 6-OHDA caused a significant decrease in green fluorescence in the mitochondria, and this was reversed by preincubation with NAD for 2 h in a dose-dependent manner. ATP production (C), and the expression of mitochondrial bioenergetic markers, including ATP6, ND1 and COX2, at the mRNA level (D, E, F) and protein level (G) were used to reflect mitochondrial bioenergetic function. The PC12 cells incubated with 200 µM 6-OHDA showed decreased ATP production accompanied by a significant compensatory increase in mitochondrial bioenergetic markers, whereas the preapplication of NAD increased ATP production and decreased the expression of mitochondrial bioenergetic markers. The values were obtained from three independent experiments. Scale bar = 100 µm. \**P* < .05, \*\**P* < .01, \*\*\**P* < .001. (For interpretation of the references to colour in this figure legend, the reader is referred to the web version of this article.)

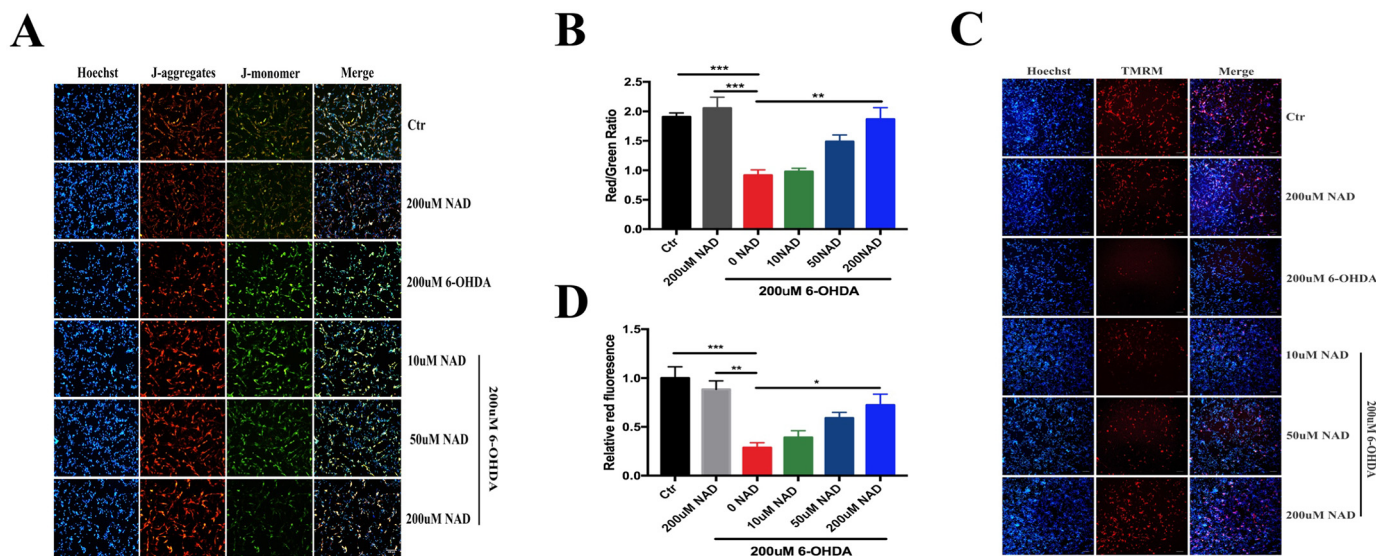


**Fig. 5.** NAD maintained the normal mitochondrial membrane potential of PC12 cells. JC-1 (A, B) and TMRM (C, D) were utilized to evaluate the mitochondrial membrane potential (MMP) of the PC12 cells at 2 h after 200  $\mu$ M 6-OHDA incubation. 6-OHDA caused a significant decrease in the number of JC-1 aggregates/monomers and red fluorescence in mitochondria, and this decrease was reversed by preincubation with NAD for 2 h in a dose-dependent manner. The values were obtained from three independent experiments. Scale bar = 100  $\mu$ m. \* $P$  < .05, \*\* $P$  < .01, \*\*\* $P$  < .001. (For interpretation of the references to colour in this figure legend, the reader is referred to the web version of this article.)

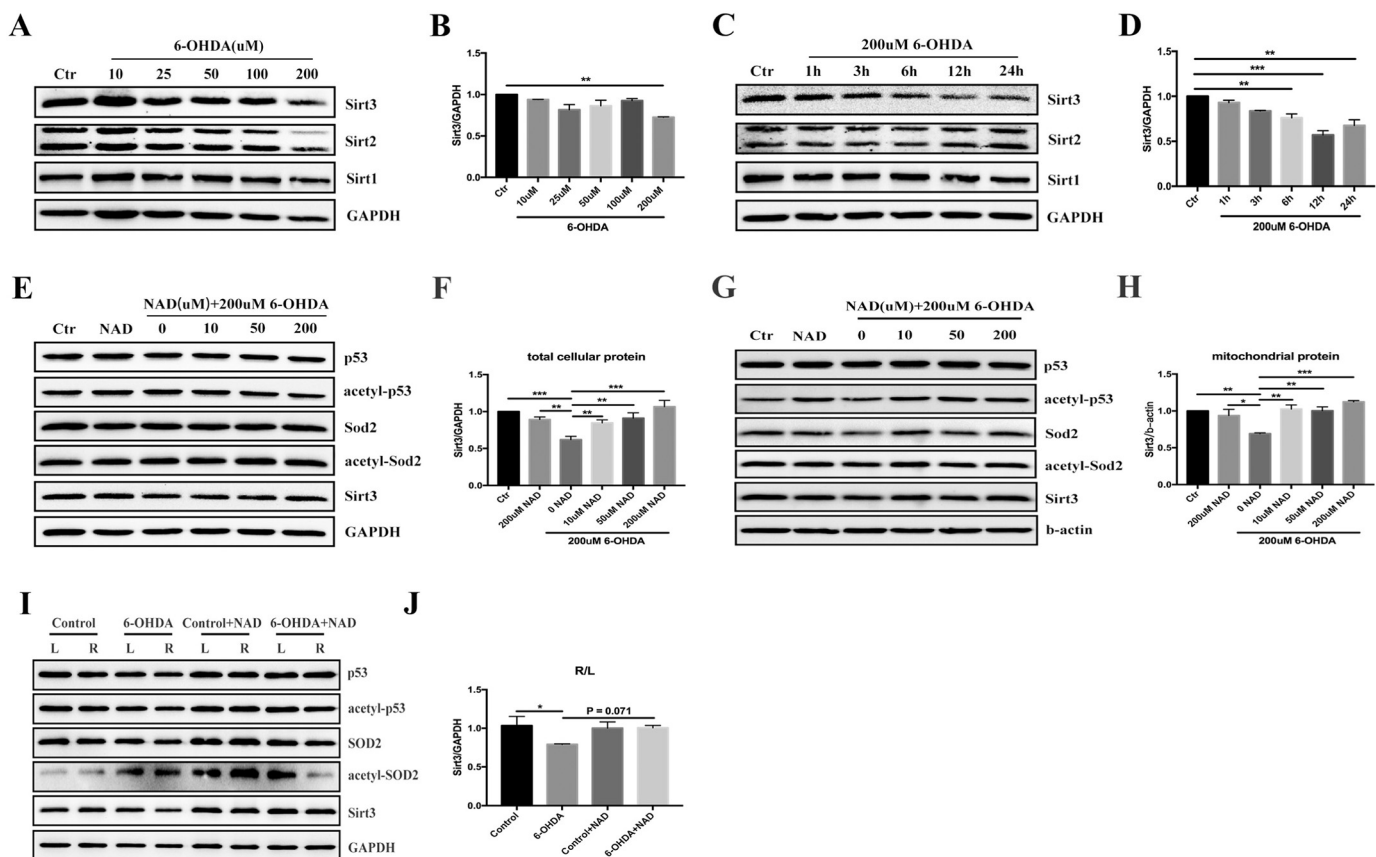


**Fig. 6.** NAD regulated Sirt3 expression in PC12 cells. 6-OHDA caused a significant decrease in Sirt3 expression at a concentration of 200  $\mu$ M (A, B), and 200  $\mu$ M 6-OHDA caused a decrease in Sirt3 expression in a time-dependent manner (C, D). 6-OHDA (200  $\mu$ M) decreased both the total protein level (E, F) and mitochondrial protein level (G, H) of Sirt3, and NAD reversed this decrease of Sirt3 in a dose-dependent manner. In vivo western blotting showed similar results (I, J). No obvious alterations were found in the expression of the Sirt3-targeted genes SOD2 and p53. The values were obtained from three independent experiments.

studies (Guo et al., 2007; Wang et al., 2003), some pieces of evidence suggested the necrosis rather than apoptosis. Beom S. Jeon et al. reported that abundant neuronal death was observed in the rat SN as early as 12 h after 6-OHDA injection and extensive neuron death continued through day 10, but at no time was the morphology of apoptosis observed (Jeon et al., 1995). Another study also found that striatal injection of 6-OHDA in mice resulted in the nuclear translocation of a hallmark of regulated necrosis, but never caused signs of apoptosis, including caspase-3 activation and cytoplasmic release of cytochrome c (Kim et al., 2011). In line with these studies, our study found that 6-OHDA injection caused the loss of TH<sup>+</sup> neurons but no obvious changes in TUNEL staining 1 week after the striatal 6-OHDA lesion (data shown in the Supplemental Fig. 2). Apoptosis refers to a form of programmed and regulated cell death mechanism that not only occurs upon cell damage or stress, but also during normal development and morphogenesis; on the contrast, necrosis is a mode of unordered and passive cellular explosion in response to acute and overwhelming trauma (Vanden Berghe et al., 2013; Nikolettou et al., 2013). Thus, considering 6-OHDA is a kind of severe chemical toxic, apoptosis may not be the dominant neuronal death pathway at least at 1 week after the 6-OHDA injection, as suggested by our study and others.

It is known that mitochondrial dysfunction is especially important in the etiology of PD and in selective dopaminergic neuronal loss in the SN (Sheng et al., 2012; Mishra et al., 2014). Because the mitochondrial NAD<sup>+</sup> pool ranges from 40% to 70% of the total cellular NAD<sup>+</sup> content (Stein et al., 2012; Cambronne et al., 2016), the mitochondrion is the most vulnerable organelle when NAD is depleted; thus, we focused on the alterations in mitochondrial function. A previous study on a *Drosophila* model of PD with a pink1 mutation found that a diet supplemented with 5 mM NAM inhibits the loss of dopaminergic neurons, possibly through maintaining normal mitochondrial morphology and respiration (Lehmann et al., 2017), revealing the protective role of NAD supplementation on the maintenance of a healthy mitochondrial pool related to PD. In the current study, we found that 6-OHDA led to reduced mitochondrial quantity along with a decreased MMP and impaired ATP production. The expression of vital proteins involved in ATP synthesis, such as COX2, ND1 and ATP6, were much higher after 6-OHDA incubation, indicating the mitochondrial injury caused by 6-OHDA treatment. Because 6-OHDA leads to a decreased mitochondrial quantity, cells may compensatorily increase the expression of mitochondrial respiratory enzyme-related molecules at the mRNA and protein levels to maintain normal energy homeostasis, resulting in the inconsistencies observed by western blotting and MitoTracker Green staining. As there is an impairment in the ability of mitochondria in the SN of PD patients to meet neuronal bioenergetic demands (Shi et al., 2017), the fact that preincubation with NAD can at least partly prevent the above phenomenon indicates that NAD may have a major role in modulating mitochondrial function to meet dopaminergic neuronal bioenergetic demands, thus preventing dopaminergic neurodegeneration.

Another potential cause of the motor deficits and pathological characteristics in PD is increased oxidative stress. Increased oxidative stress is one of the prominent features of PD and is either as a primary cause or a secondary component of the pathophysiology (Coskun et al., 2012; Schapira et al., 2014; Bose et al., 2016). It leads to the accumulation of cytotoxic compounds that result not only in protein collapse, enzyme failure and lipid destruction (Lee et al., 2012) but also in the destruction of a majority of dopaminergic neurons (Shukla et al., 2011) and a reduction in the antioxidant enzyme barrier (Jiang et al., 2016). In line with previous studies (Singh et al., 2016; Prajapati et al., 2017), 6-OHDA injection caused a striking increase in ROS levels and a significant decrease in SOD activity in PC12 cells, and these changes were prominently reversed by preincubation with NAD. This result explains why NAD can alleviate 6-OHDA-induced mitochondrial dysfunction in PC12 cells and dopaminergic neuron loss in the nigrostriatal system.

Sirt3, the most abundant sirtuin in the brain, localizes to the mitochondrial inner membrane, the mitochondrial matrix and the nucleus of neurons (Onyango et al., 2002), and may mediate the connection between mitochondrial dysfunction and the loss of dopaminergic neurons in the SN of patients with PD. It can deacetylate diverse substrates to affect distinct aspects of mitochondrial function, including ATP production (Rahman et al., 2014), electron transport chain activity (Ahn et al., 2008), and amino acid metabolism (Hallows et al., 2011). Indeed, the genetic deletion of Sirt3 increases oxidative stress and decreases the membrane potential of mitochondria in SN dopaminergic neurons, which is attributed to increased acetylation and the decreased activity of SOD (Shi et al., 2017). In addition, Sirt3 deficiency dramatically exacerbates the degeneration of nigrostriatal dopaminergic neurons in 1-methyl-4-phenyl-1,2,3,6-tetrahydropyridine (MPTP)-induced PD mice, possibly via decreased levels of SOD2 and glutathione peroxidase (Liu et al., 2015). In addition, it has been found to prevent p53-induced mitochondrial dysfunction and neuronal damage in a deacetylase activity-dependent manner, and thus has therapeutic potential to ameliorate mitochondrial pathology and neurodegeneration in AD (Lee et al., 2018). These findings prompted us to focus on the function of Sirt3 in PD. In the current study, 6-OHDA treatment caused a significant decrease in Sirt3 expression both in vivo and in vitro, and pretreatment with NAD partly reversed this decrease, indicating that the protective effects of NAD may be mediated via Sirt3. However, we did not find any obvious alterations in the Sirt3-targeted downstream proteins p53 and SOD2. This may be attributed to the reason that the role of NAD is more relevant to PD pathogenesis than to the function of Sirt3 in neurotoxicity-induced dopaminergic neuronal damage because neurotoxicity-induced dopaminergic neuronal death cannot completely replicate the dopaminergic neurodegeneration observed in PD (Shi et al., 2017).

One intriguing question worthy of discussion is to what extent was the used amount of NAD in vivo in comparable with the observed dose-dependence in vitro. Given that the molecular weight of NAD is 685.41, the estimated volume of ST is around 4 mm × 2.25 mm × 3 mm based on the stereotaxic coordinates of the mouse brain, and the absorbance rate is 100% as we injected NAD directly into ST, the comparable amount with 200 μM NAD, which was the most beneficial concentration in vitro, is about 4 μg in vivo. Our preliminary experiments in vivo, in which 4 μg, 20 μg and 100 μg NAD were pre-injected into the right ST of mice respectively, found that 20 μg was the lower dose which was effective in preventing TH<sup>+</sup> dopaminergic neuronal loss (data not shown), so we chose 20 μg as the dose of NAD for our formal in vivo experiments. Although we have demonstrated the protective effects of NAD against motor deficits and dopaminergic neurodegeneration in PD mice and 6-OHDA-induced oxidative stress and mitochondrial dysfunction in PC12 cells in the current study, there are still some questions worthy of further exploration. Our study mainly focused on the modulation of bioenergetic defects in the protective effects of NAD on mitochondrial function. As most mitochondrial function is determined by the balance between fusion and fission (Franco-Iborra et al., 2016), further studies are needed to study the effect of NAD on mitochondrial dynamics, morphology and trafficking or transport. In addition, we did not inhibit the expression and activity of Sirt3 with its inhibitor 3-TYP, so further studies are needed to confirm that NAD exerts its protective effects in PC12 cells and PD mice via Sirt3.

## 5. Conclusion

Based on previously the reported neuroprotective effects of NAD in other neurodegenerative diseases and the good tolerance of its precursors for treating cardiovascular and other physiological functions in aging humans (Martens et al., 2018), our study adds credence to the beneficial role of NAD in models of neurodegeneration and suggests the potential of NAD in the prevention of PD.

## Funding

This work was supported by the National Natural Science Foundation of China [grant numbers 81870619, 81570796 and 81871064]; the National Key Research and Development Program of China [grant number 2016YFC1201701]; the Shanghai Committee of Science and Technology [grant number 13dz2260500]; and the Innovation Program of Shanghai Municipal Education Commission [grant number 2019-01-07-00-02-E00037].

## Conflict of interests

The authors declare no conflict of interest.

## Authors contributions

CS conducted the main experiments and wrote the manuscript. YG and QZ performed the western blotting and analyzed the data; YH and SW obtained the brain slices and performed the immunohistochemistry; QZ and GH were responsible for the mitochondrial studies; BT, LS and HZ were responsible for NAD, SOD, ROS and ATP detection. SL and JL conceived the idea and revised the manuscript.

## Ethical statement

All animal experiments in this study were approved by the ethics committee of Shanghai Jiao Tong University (SJTU) and conducted according to the National Institutes of Health Guidelines for the Care and Use of Laboratory Animals (NIH Publications No. 8023, revised 1978).

## Supplementary data

Supplementary data to this article can be found online at <https://doi.org/10.1016/j.pnpbp.2019.109670>.

## References

Ahn, B.H., et al., 2008. A role for the mitochondrial deacetylase Sirt3 in regulating energy homeostasis. *Proc. Natl. Acad. Sci. U. S. A.* 105, 14447–14452.

Alano, C.C., et al., 2010. NAD<sup>+</sup> depletion is necessary and sufficient for poly(ADP-ribose) polymerase-1-mediated neuronal death. *J. Neurosci.* 30, 2967–2978.

Anderson, G., et al., 2014. Neurodegeneration in Parkinson's disease: interactions of oxidative stress, tryptophan catabolites and depression with mitochondria and sirtuins. *Mol. Neurobiol.* 49, 771–783.

Bai, P., et al., 2011. PARP-1 inhibition increases mitochondrial metabolism through SIRT1 activation. *Cell Metab.* 13, 461–468.

Berger, F., et al., 2004. The new life of a centenarian: signalling functions of NAD(P). *Trends Biochem. Sci.* 29, 111–118.

Blandini, F., et al., 2000. Functional changes of the basal ganglia circuitry in Parkinson's disease. *Prog. Neurobiol.* 62, 63–88.

Bose, A., et al., 2016. Mitochondrial dysfunction in Parkinson's disease. *J. Neurochem.* 139 (Suppl. 1), 216–231.

Calabresi, P., et al., 2013. New experimental and clinical links between the hippocampus and the dopaminergic system in Parkinson's disease. *Lancet Neurol.* 12, 811–821.

Cambronne, X.A., et al., 2016. Biosensor reveals multiple sources for mitochondrial NAD<sup>+</sup>. *Science* 352, 1474–1477.

Coskun, P., et al., 2012. A mitochondrial etiology of Alzheimer and Parkinson disease. *Biochim. Biophys. Acta* 1820, 553–564.

Dauer, W., et al., 2003. Parkinson's disease: mechanisms and models. *Neuron* 39, 889–909.

Delgado-Camprubi, M., et al., 2017. Deficiency of Parkinson's disease-related gene Fbxo7 is associated with impaired mitochondrial metabolism by PARP activation. *Cell Death Differ.* 24, 120–131.

Donmez, G., 2012. The neurobiology of sirtuins and their role in neurodegeneration. *Trends Pharmacol. Sci.* 33, 494–501.

Fang, E.F., et al., 2016. NAD<sup>+</sup> replenishment improves lifespan and healthspan in Ataxia telangiectasia models via mitophagy and DNA repair. *Cell Metab.* 24, 566–581.

Fang, E.F., et al., 2017. NAD<sup>+</sup> in aging: molecular mechanisms and translational implications. *Trends Mol. Med.* 23, 899–916.

Fearnley, J.M., et al., 1991. Ageing and Parkinson's disease: substantia nigra regional selectivity. *Brain* 114 (Pt 5), 2283–2301.

Franco-Iborra, S., et al., 2016. The Parkinson disease mitochondrial hypothesis: where are

we at? *Neuroscientist* 22, 266–277.

Frezza, C., et al., 2007. Organelle isolation: functional mitochondria from mouse liver, muscle and cultured fibroblasts. *Nat. Protoc.* 2, 287–295.

Gong, B., et al., 2013. Nicotinamide riboside restores cognition through an upregulation of proliferator-activated receptor-gamma coactivator 1alpha regulated beta-secretase 1 degradation and mitochondrial gene expression in Alzheimer's mouse models. *Neurobiol. Aging* 34, 1581–1588.

Guo, S., et al., 2007. Protective effects of green tea polyphenols in the 6-OHDA rat model of Parkinson's disease through inhibition of ROS-NO pathway. *Biol. Psychiatry* 62, 1353–1362.

Guo, X., et al., 2017. FGF18 protects against 6-hydroxydopamine-induced nigrostriatal damage in a rat model of Parkinson's disease. *Neuroscience* 356, 229–241.

Guo, X.Z., et al., 2018. Osteocalcin ameliorates motor dysfunction in a 6-hydroxydopamine-induced Parkinson's disease rat model through AKT/GSK3beta signaling. *Front. Mol. Neurosci.* 11, 343.

Hallows, W.C., et al., 2011. Sirt3 promotes the urea cycle and fatty acid oxidation during dietary restriction. *Mol. Cell* 41, 139–149.

Imai, S., et al., 2014. NAD<sup>+</sup> and sirtuins in aging and disease. *Trends Cell Biol.* 24, 464–471.

Jeon, B.S., et al., 1995. 6-Hydroxydopamine lesion of the rat substantia nigra: time course and morphology of cell death. *Neurodegeneration* 4, 131–137.

Jiang, T., et al., 2016. Oxidative stress: a major pathogenesis and potential therapeutic target of antioxidative agents in Parkinson's disease and Alzheimer's disease. *Prog. Neurobiol.* 147, 1–19.

Kim, T.W., et al., 2011. Dissociation of progressive dopaminergic neuronal death and behavioral impairments by Bax deletion in a mouse model of Parkinson's diseases. *PLoS One* 6, e25346.

Kruger, R., et al., 2017. Classification of advanced stages of Parkinson's disease: translation into stratified treatments. *J. Neural Transm. (Vienna)* 124, 1015–1027.

Lee, D.H., et al., 2012. Mechanisms of oxidative damage in multiple sclerosis and neurodegenerative diseases: therapeutic modulation via fumaric acid esters. *Int. J. Mol. Sci.* 13, 11783–11803.

Lee, J., et al., 2018. SIRT3 deregulation is linked to mitochondrial dysfunction in Alzheimer's disease. *Aging Cell* 17.

Lehmann, S., et al., 2016. Parp mutations protect against mitochondrial dysfunction and neurodegeneration in a PARKIN model of Parkinson's disease. *Cell Death Dis.* 7, e2166.

Lehmann, S., et al., 2017. Enhancing NAD<sup>+</sup> salvage metabolism is neuroprotective in a PINK1 model of Parkinson's disease. *Biol. Open* 6, 141–147.

Liu, L., et al., 2015. SIRT3 attenuates MPTP-induced nigrostriatal degeneration via enhancing mitochondrial antioxidant capacity. *Neurochem. Res.* 40, 600–608.

Lu, L., et al., 2014. Nicotinamide mononucleotide improves energy activity and survival rate in an in vitro model of Parkinson's disease. *Exp. Ther. Med.* 8, 943–950.

Martens, C.R., et al., 2018. Chronic nicotinamide riboside supplementation is well-tolerated and elevates NAD<sup>+</sup> in healthy middle-aged and older adults. *Nat. Commun.* 9, 1286.

Michishita, E., et al., 2005. Evolutionarily conserved and nonconserved cellular localizations and functions of human SIRT proteins. *Mol. Biol. Cell* 16, 4623–4635.

Mishra, P., et al., 2014. Mitochondrial dynamics and inheritance during cell division, development and disease. *Nat. Rev. Mol. Cell Biol.* 15, 634–646.

Mouchiroud, L., et al., 2013. The NAD<sup>+</sup>/Sirtuin pathway modulates longevity through activation of mitochondrial UPR and FOXO signaling. *Cell* 154, 430–441.

Nikoletopoulou, V., et al., 2013. Crosstalk between apoptosis and autophagy. *Biochim. Biophys. Acta* 1833, 3448–3459.

Onyango, P., et al., 2002. SIRT3, a human SIR2 homologue, is an NAD-dependent deacetylase localized to mitochondria. *Proc. Natl. Acad. Sci. U. S. A.* 99, 13653–13658.

Outeiro, T.F., et al., 2007. Sirtuin 2 inhibitors rescue alpha-synuclein-mediated toxicity in models of Parkinson's disease. *Science* 317, 516–519.

Peelaerts, W., et al., 2016. a-Synuclein strains and the variable pathologies of synucleinopathies. *J. Neurochem.* 139 (Suppl. 1), 256–274.

Pehar, M., et al., 2018. Nicotinamide adenine dinucleotide metabolism and neurodegeneration. *Antioxid. Redox Signal.* 28, 1652–1668.

Peng, K., et al., 2017. The interaction of mitochondrial biogenesis and fission/fusion mediated by PGC-1alpha regulates rotenone-induced dopaminergic neurotoxicity. *Mol. Neurobiol.* 54, 3783–3797.

Prajapati, S.K., et al., 2017. Coenzyme Q10 prevents mitochondrial dysfunction and facilitates pharmacological activity of atorvastatin in 6-OHDA induced dopaminergic toxicity in rats. *Neurotox. Res.* 31, 478–492.

Przedborski, S., et al., 1995. Dose-dependent lesions of the dopaminergic nigrostriatal pathway induced by intrastriatal injection of 6-hydroxydopamine. *Neuroscience* 67, 631–647.

Rahman, M., et al., 2014. Drosophila Sirt2/mammalian SIRT3 deacetylates ATP synthase beta and regulates complex V activity. *J. Cell Biol.* 206, 289–305.

Rozas, G., et al., 1998. The overall rod performance test in the MPTP-treated-mouse model of parkinsonism. *J. Neurosci. Methods* 83, 165–175.

Schallert, T., et al., 2000. CNS plasticity and assessment of forelimb sensorimotor outcome in unilateral rat models of stroke, cortical ablation, parkinsonism and spinal cord injury. *Neuropharmacology* 39, 777–787.

Schapiro, A.H., et al., 2014. Slowing of neurodegeneration in Parkinson's disease and Huntington's disease: future therapeutic perspectives. *Lancet* 384, 545–555.

Schondorf, D.C., et al., 2018. The NAD<sup>+</sup> precursor nicotinamide riboside rescues mitochondrial defects and neuronal loss in iPSC and fly models of Parkinson's disease. *Cell Rep.* 23, 2976–2988.

Sheng, Z.H., et al., 2012. Mitochondrial transport in neurons: impact on synaptic homeostasis and neurodegeneration. *Nat. Rev. Neurosci.* 13, 77–93.

Shi, H., et al., 2017. Sirt3 protects dopaminergic neurons from mitochondrial oxidative

- stress. *Hum. Mol. Genet.* 26, 1915–1926.
- Shukla, V., et al., 2011. Oxidative stress in neurodegeneration. *Adv. Pharmacol. Sci.* 2011, 572634.
- Singh, S., et al., 2016. ALCAR exerts neuroprotective and pro-neurogenic effects by inhibition of glial activation and oxidative stress via activation of the Wnt/beta-catenin signaling in parkinsonian rats. *Mol. Neurobiol.* 53, 4286–4301.
- Soto-Otero, R., et al., 2000. Autoxidation and neurotoxicity of 6-hydroxydopamine in the presence of some antioxidants: potential implication in relation to the pathogenesis of Parkinson's disease. *J. Neurochem.* 74, 1605–1612.
- Stein, L.R., et al., 2012. The dynamic regulation of NAD metabolism in mitochondria. *Trends Endocrinol. Metab.* 23, 420–428.
- Szego, E.M., et al., 2017. Sirtuin 2 enhances dopaminergic differentiation via the AKT/GSK-3beta/beta-catenin pathway. *Neurobiol. Aging* 56, 7–16.
- Vanden Berghe, T., et al., 2013. Determination of apoptosis and necrotic cell death in vitro and in vivo. *Methods* 61, 117–129.
- Verdin, E., 2015. NAD(+) in aging, metabolism, and neurodegeneration. *Science* 350, 1208–1213.
- Walsh, R.N., et al., 1976. The open-field test: a critical review. *Psychol. Bull.* 83, 482–504.
- Wang, Y., et al., 2003. Diadenosine tetraphosphate protects against injuries induced by ischemia and 6-hydroxydopamine in rat brain. *J. Neurosci.* 23, 7958–7965.
- Wareski, P., et al., 2009. PGC-1 $\alpha$  and PGC-1 $\beta$  regulate mitochondrial density in neurons. *J. Biol. Chem.* 284, 21379–21385.
- Wu, J., et al., 2017. Redox imbalance and mitochondrial abnormalities in the diabetic lung. *Redox Biol.* 11, 51–59.
- Zhou, M., et al., 2015. Neuronal death induced by misfolded prion protein is due to NAD<sup>+</sup> depletion and can be relieved in vitro and in vivo by NAD<sup>+</sup> replenishment. *Brain* 138, 992–1008.
- Zhou, T., et al., 2016. Neuroprotective effects of ginsenoside Rg1 through the Wnt/beta-catenin signaling pathway in both in vivo and in vitro models of Parkinson's disease. *Neuropharmacology* 101, 480–489.
- Zhu, X.J., et al., 2009. The effects of BAFF and BAFF-R-Fc fusion protein in immune thrombocytopenia. *Blood* 114, 5362–5367.
- Zhu, X.H., et al., 2015. In vivo NAD assay reveals the intracellular NAD contents and redox state in healthy human brain and their age dependences. *Proc. Natl. Acad. Sci. U. S. A.* 112, 2876–2881.